Effects of spin polarization on the structural and electronic properties of supercritical fluid selenium: *ab initio* molecular-dynamics simulations

1999 J. Phys.: Condens. Matter 11 8829

(http://iopscience.iop.org/0953-8984/11/45/307)

J. Phys.: Condens. Matter **11** (1999) 8829–8838. Printed in the UK PII: S0953-8984(99)07195-7

Effects of spin polarization on the structural and electronic properties of supercritical fluid selenium: *ab initio* molecular-dynamics simulations

Fuyuki Shimojo†, Kozo Hoshino† and Y Zempo‡

† Faculty of Integrated Arts and Sciences, Hiroshima University, Higashi–Hiroshima 739-8521, Japan

‡ Sumitomo Chemical, 6 Kitahara, Tsukuba 300-3294, Japan

Received 24 August 1999

Abstract. The effects of spin polarization on the atomic and electronic structures of supercritical fluid selenium are investigated by means of *ab initio* molecular-dynamics simulations using the fully spin-polarized and generalized-gradient-corrected density functional theory. Detailed investigations of the density dependence of the electronic density of states and the pair distribution functions show that the spin polarization plays a crucially important role in determining the properties of supercritical fluid selenium. It is confirmed from the spatial distribution of the spin density that there is a strong correlation between the chain structure and the amount of spin polarization around each Se atom.

1. Introduction

Near the triple point, liquid Se consists of large chain molecules and exhibits semiconducting properties [1]. Each molecule includes 10^5 atoms on average [2, 3]. With increases in the temperature and the pressure, the electrical conductivity increases gradually [4, 5], and a metallic state appears near the critical point (the critical temperature T_c, pressure P_c and density d_c are 1863 K, 380 bar [4] and 1.85 g cm^{-3} [6], respectively). It has been confirmed both experimentally [7–9] and theoretically [10] that the chain-like structure remains even in the metallic state although the average chain length decreases substantially; it approaches only about ten atoms near the critical point [7]. An *ab initio* molecular-dynamics (MD) study [10] showed that the shortening of Se chains is responsible for the metallization. When the Se–Se bonds in chain molecules break, the anti-bonding states above the Fermi level (ε_F) are stabilized while the bonding or the non-bonding states below ε_F become unstable, and, therefore, the gap at ε_F disappears at high temperatures.

When the pressure is decreased from the metallic state, keeping the temperature higher than T_c, the metallic properties disappear, and finally fluid Se goes into a vapour phase which consists of Se_2 dimers. Recently, Tamura and collaborators [11, 12] carried out XAFS measurements for fluid Se in this supercritical region to investigate the change of the atomic structure with decreasing pressure, and the mechanism by which the vapour phase appears from the metallic phase.

Several *ab initio* MD simulations have been carried out for liquid Se under conditions with the density $d > d_c$ and the temperature $T < T_c$, including the metallic state [10, 13–15]. In all of these simulations, the spin polarization is neglected, and the electronic states are constrained

0953-8984/99/458829+10$30.00

to be either doubly occupied or unoccupied. At relatively high densities, this approximation does not have significant influence on the properties of liquid Se [15]. However, the effects of the spin polarization will become important with decreasing density. We expected, for the supercritical region with $d < d_c$, the spin polarization of each short chain to play a crucial role in determining the electronic and structural properties of fluid Se, because Se chains are distant from each other, and are almost isolated. To see the importance of the spin polarization, the obvious choice is to consider the vapour phase; degenerate $\pi_g(x)$ and $\pi_g(y)$ states in the Se_2 dimer are occupied by electrons with the same direction of spin polarization, and, therefore, the electronic structure of the Se_2 dimer can be reproduced only when we take into account the spin polarization. Otherwise the electronic density of states has a sharp peak at ε_F as will be shown later, which is at variance with the fact that the vapour phase is an insulator.

In this paper, we report the results of *ab initio* MD simulations for fluid Se in the supercritical region with $d < d_c$ and $T > T_c$. We perform full spin-polarized calculations. The purposes of our MD simulations are (i) to investigate the effects of the spin polarization on the electronic and structural properties of supercritical fluid Se and (ii) to clarify how the structure of fluid Se changes when the pressure is decreased in the supercritical region. The method of calculation is described briefly in section 2. The results of our simulation and discussions are given in section 3. Finally section 4 summarizes our work.

2. Method of calculation

Our calculations are performed within the framework of the density functional theory (DFT). The generalized-gradient approximation is used for the exchange–correlation energy in fully spin-polarized form [16]. The electronic wavefunctions are expanded in the plane-wave (PW) basis set. The energy functional is minimized using an iterative scheme based on the preconditioned conjugate-gradient method [17–19]. For the valence electron–ion interaction, we used the ultrasoft pseudopotential proposed by Vanderbilt [20, 21].

In our previous calculations [10], we used the cubic supercell which contains 81 Se atoms, with periodic boundary conditions. Three simulations were carried out at different temperatures T (K) and densities d (g cm^{-3}): $(T, d) = (870, 3.75)$, (1170, 3.54) and (1770, 3.33). The states at two temperatures, 870 and 1170 K, are in the semiconducting region, while the state at 1770 K is in the metallic region. In the present study, we carry out MD simulations for two states in the supercritical region: $(T, d) = (1920, 2.0)$ and (1920, 1.0). Since the number of basis functions needed for the electronic structure calculations is proportional to $1/d$, the present calculations are more expensive as regards computation time than the previous three simulations. For this reason, we utilize a system of 64 atoms in a cubic supercell. Though the number of atoms is smaller than that in the previous study [10], it is acceptable because the system consists of only short Se chains for the thermodynamic states with which we are concerned here. For the state at $(T, d) = (1920, 1.0)$, a MD simulation using the spin-unpolarized DFT is also carried out to investigate the effects of the spin polarization on the properties of fluid Se.

Using the Nosé–Hoover thermostat technique [22, 23], the equations of motion are solved via the velocity Verlet algorithm with a time step $\Delta t = 1.7$ fs. The Γ point is used for the Brillouin-zone sampling, and the PW cut-off energies for the wavefunctions and the charge density are 11 and 55 Ryd, respectively. The initial charge density at each MD step is estimated by extrapolating the charge densities at the preceding steps [19], and the initial wavefunctions are estimated from the wavefunctions at the preceding steps by a subspace diagonalization [18]. The quantities of interest are obtained by averaging over about 1000 Δt after the initial equilibration taking at least 300 Δt.

3. Results and discussion

3.1. Effects of the spin polarization on the bond breaking in an isolated Se chain

Before we show the results of MD simulations for supercritical fluid Se, we describe the effects of the spin polarization on the bond breaking in an isolated Se chain. Since the bond breaking and the rearrangement of Se chains occur frequently in fluid Se, it is useful and important to clarify the role of the spin polarization using a simple model in order to understand the dynamic properties of fluid Se. Using the same method as described in the preceding section, we calculate the electronic structure of an isolated infinite Se chain, which is assumed to have a threefold screw rotation symmetry. The hexagonal supercell contains six Se atoms, and the rotation axis of the Se chain is along the c-direction of the supercell. The lengths of the supercell edges in the xy-plane are fixed at $a = 7$ Å, which is large enough to separate the chain from the neighbouring chains. When the total energy is calculated as a function of the length of the supercell edge c by relaxing the atomic positions so as to minimize the total energy, the minimum energy is obtained at $c = 9.6$ Å. The geometrical parameters are the bond length $\ell_0 = 2.37$ Å, the bond angle $\theta = 100.7^\circ$ and the dihedral angle $\phi = 96.7^\circ$, which are compared with the experimental values of $\ell_0 = 2.37$ Å, $\theta = 103^\circ$ and $\phi = 101^\circ$ for crystalline trigonal Se [24] and $\ell_0 = 2.34$ Å, $\theta = 102^\circ$ and $\phi = 75^\circ$ for the Se chain confined in the channel of mordenite [25]. Although the geometrical parameters that we have obtained are not for the ground state of the isolated infinite chain, we use this model. It is adequate for investigating the effects of the spin polarization on the bond breaking in a Se chain qualitatively.

To simulate the bond breaking in a Se chain, the length of c is increased, while the geometrical parameters are fixed except for a Se–Se bond, which is hereafter called the stretched bond. The electronic structure is obtained by using both spin-polarized and spin-unpolarized DFTs. Figure 1 shows the single-electron eigenvalues ε_i near the Fermi level ($\varepsilon_F = 0$) as a function of $\ell_{sep} = \ell/\ell_0$, with ℓ and ℓ_0 being the bond length of the stretched bond and the equilibrium bond length, respectively. Figures 1(a) and 1(b) are obtained using the spin-

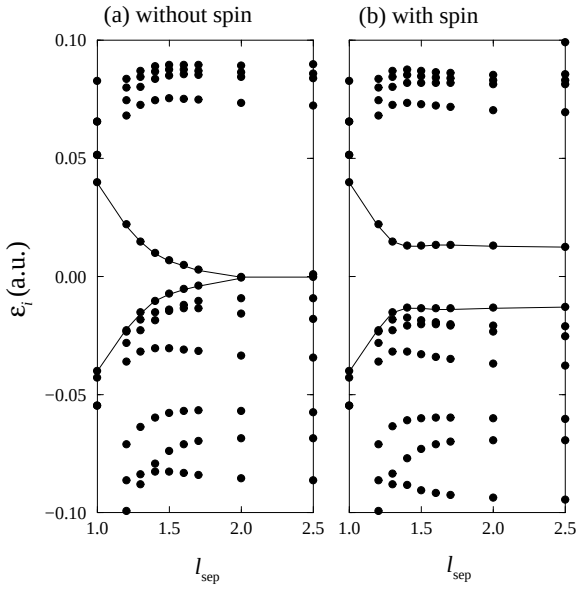

Figure 1. Single-electron eigenvalues ε_i of the Se_6 chain as a function of $\ell_{sep} = \ell/\ell_0$ with ℓ and ℓ_0 being the bond length of the stretched bond and the equilibrium bond length, respectively, obtained from (a) spin-unpolarized DFT and (b) spin-polarized DFT. The lines in each panel are drawn as guides to the eyes.

unpolarized and the spin-polarized DFTs, respectively. As is clearly seen in these figures, the main differences are as regards the $\ell_{\rm sep}$-dependencies of the HOMO (highest occupied molecular orbital) and LUMO (lowest unoccupied molecular orbital). Since the unoccupied LUMO is characterized by anti-bonding states, it would be stabilized by the bond breaking [26]. This is why the ε_i for the LUMO approach those for the HOMO with increasing $\ell_{\rm sep}$. In the spin-unpolarized case, this mechanism is operative for all $\ell_{\rm sep}$, and finally the HOMO and the LUMO become degenerate for $\ell_{\rm sep} > 2$. Ohtani *et al* [27] have carried out an electronic structure calculation for this model without taking into account the spin polarization and obtained the same results as the present work. On the other hand, in the spin-polarized case, the HOMO and the LUMO never become degenerate, and there is a gap even for large $\ell_{\rm sep}$, because the spin polarization occurs at the ends of the Se chain as shown in figure 2, where the spin density (=the difference between the up- and the down-spin electron densities) is plotted as well as the total electron density.

The spin polarization affects not only the single-electron eigenvalues but also the atomic

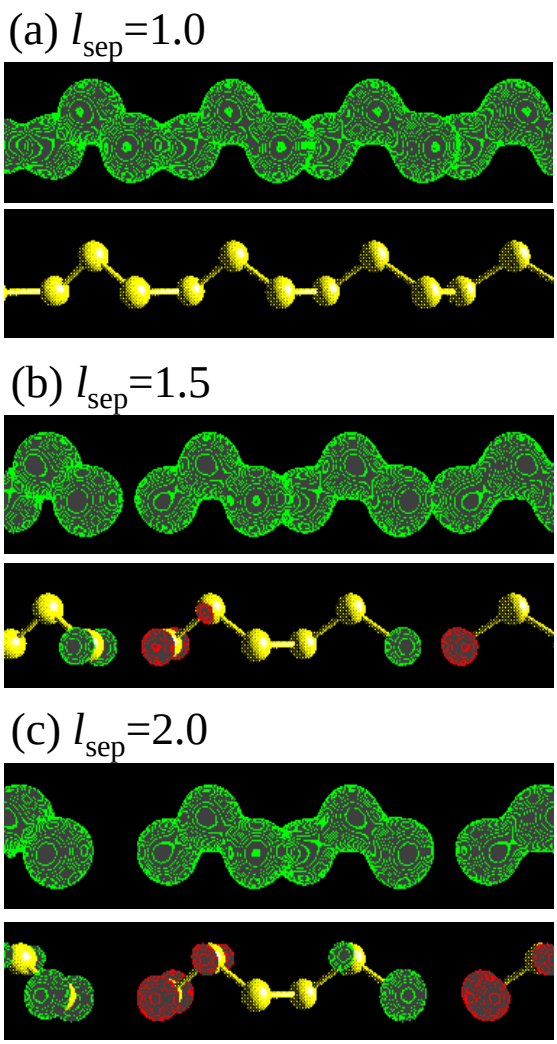

Figure 2. The total electron density $\rho(\boldsymbol{r})$ (upper portion in each panel) and spin density $\sigma(\boldsymbol{r})$ (lower portion in each panel) for $\ell_{\rm sep}$ = (a) 1.0, (b) 1.5 and (c) 2.0 obtained from the spin-polarized DFT. In the upper portion in each panel, the isosurface of $\rho(\boldsymbol{r}) = 0.05$ au is plotted, while the lower portion shows the isosurface of $|\sigma(\boldsymbol{r})| = 0.01$ au; different degrees of shading indicate different signs of $\sigma(\boldsymbol{r})$.

forces. We calculate the atomic force acting on the atoms at the ends of the Se chain, and display the component F_b along the stretched bond in figure 3 as a function of ℓ_{sep}. The positive values of F_b mean that the attractive force acts on the atoms. For $\ell_{sep} < 1.3$, there is no discrepancy between the spin-polarized and the spin-unpolarized cases. However, for $\ell_{sep} > 1.3$, there are significant differences between them; e.g. at $\ell_{sep} = 1.5$, a repulsive force is acting on the atoms in the spin-polarized case, while the force is still attractive in the spin-unpolarized case. $\ell_{sep} = 1.3$ corresponds to the distance of 3.1 Å, which seldom occurs in liquid Se up to the metallic phase but occurs frequently in the supercritical region with $d < d_c$.

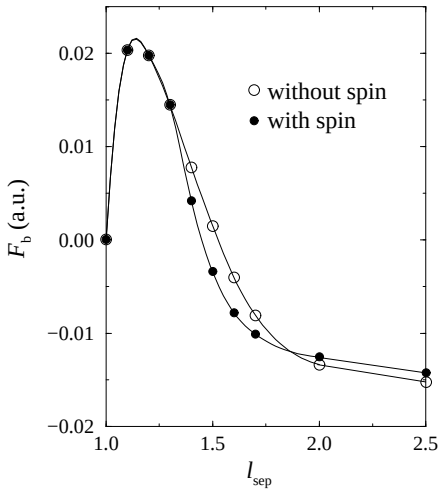

Figure 3. The atomic force F_b acting on the atoms at the ends of the Se_6 chain, which is projected onto the stretched bond. The solid and open circles show F_b obtained from the spin-polarized and the spin-unpolarized DFTs, respectively.

3.2. Electronic structure of supercritical fluid Se

Figure 4 shows the density dependence of the electronic density of states (DOS) $D(\varepsilon)$ in fluid Se, which is obtained from a time average of the distribution of the single-electron eigenvalues. In the figure, the DOSs in the supercritical region are compared with those in the semiconducting (870 K) and metallic (1770 K) phases.

The electronic structure of fluid Se in the semiconducting phase is similar to that of trigonal Se, as shown in figure 4(a), which means that the chain-like structure is largely preserved, even though the temperature is rather high compared with the melting temperature. The electronic states below -10 eV are s-like in character, while those above -7 eV are p-like. The peaks at around -15 and -11 eV correspond to s-like bonding and s-like anti-bonding states, respectively. The p-like states are decomposed into three states; the electronic states between -7 and -3 eV show p-like bonding, those between -3 and 0 eV show p-like non-bonding and those above 0 eV show p-like anti-bonding. There is a dip at ε_F in the DOS instead of a gap, because the chain structure is fairly disrupted. In the metallic phase (figure 4(b)), the overall profile of the DOS is unchanged, although there is no distinction between the p-like non-bonding and the p-like anti-bonding states. This is caused by the chain-like structure persisting even in the metallic state.

When the density is decreased to 2.0 g cm^{-3}, the overall profile still does not change, as shown in figure 4(c). It is, however, noted that the dip appears again at ε_F. At the density of

1.0 g cm^{-3} (figure 4(d)), the DOS is substantially different from those at other densities; the dip at ε_F becomes much deeper, and there appear sharp peaks in the DOS which correspond to the energy levels of the Se_2 dimer. The appearance of the dip at ε_F is consistent with the fact that these states are observed as insulators.

To investigate the effects of the spin polarization on the electronic structure of fluid Se, we show the DOSs obtained using the spin-polarized and the spin-unpolarized DFTs in figure 5. If the spin polarization is not considered, there is a sharp peak at ε_F instead of the dip, which is due to the same effects as are demonstrated by the calculation for the isolated Se chain (see figure 1). Taking into account the spin polarization, the sharp peak at ε_F splits into two peaks as shown by the bold line in figure 5. It is concluded from these calculations that the metal–insulator transition observed in supercritical fluid Se is never reproduced by the spin-unpolarized theories, and that the spin polarization plays an extremely important role in reproducing the electronic structure of fluid Se in the supercritical region with densities $\leqslant$1.0 g cm^{-3}.

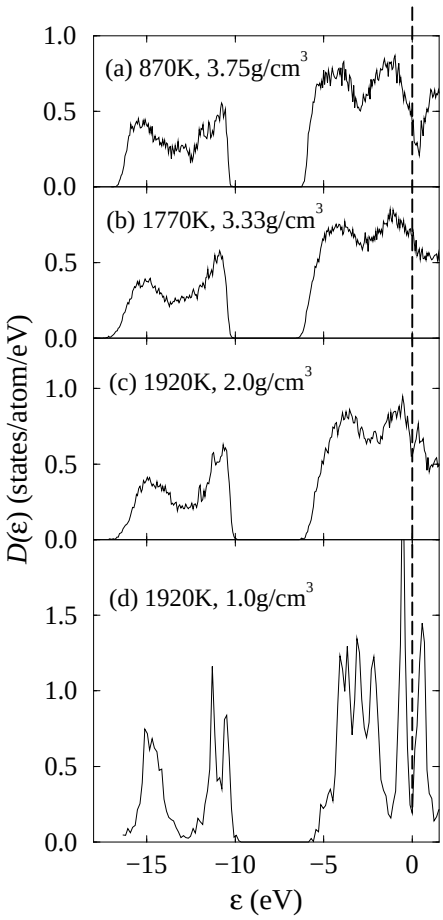

Figure 4. Electronic densities of states $D(\varepsilon)$ of fluid Se for (temperature (K), density (g cm^{-3})) = (a) (870, 3.75), (b) (1770, 3.33), (c) (1920, 2.0) and (d) (1920, 1.0). The dashed line shows the Fermi level ($\varepsilon_F = 0$).

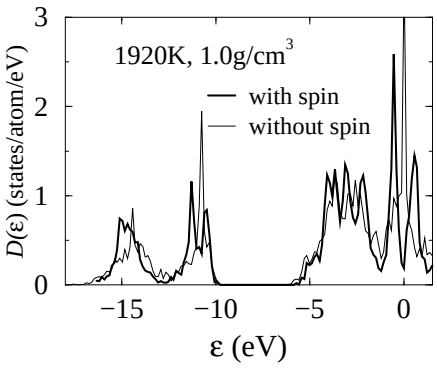

Figure 5. Electronic densities of states $D(\varepsilon)$ of fluid Se for 1920 K and 1.0 g cm^{-3}. The bold and thin lines show $D(\varepsilon)$ obtained from the spin-polarized and the spin-unpolarized DFTs, respectively.

3.3. Atomic structure of supercritical fluid Se

Figure 6 shows the calculated pair distribution functions $g(r)$ of fluid Se. When the pressure is decreased in the supercritical region, the height of the first peak of $g(r)$ becomes higher and its position r_1 moves to smaller r with decreasing density, as shown in figure 6. The values of r_1 are 2.32, 2.30 and 2.20 Å at 3.33, 2.0 and 1.0 g cm^{-3}, respectively. It is considered that r_1 will approach the bond distance 2.17 Å of the Se_2 dimer in the vapour phase. The coordination number N_1, which is estimated here from the formula

$$2\rho \int_0^{r_1} 4\pi r^2 g(r)\,\mathrm{d}r$$

with ρ being the number density of atoms, decreases as the density decreases. The values of N_1 are 1.5, 1.24 and 1.08 for the densities 3.33, 2.0 and 1.0 g cm^{-3}, respectively. The density dependencies of r_1 and N_1 are consistent with the XAFS measurements [11, 12].

To examine the effects of the spin polarization on the atomic structure, we show the $g(r)$s obtained using the spin-polarized and the spin-unpolarized DFTs in figure 7. If the spin polarization is not taken into account, the height of the first peak is 8.2 and its position is at 2.25 Å; these values are, respectively, lower and larger than the height of 11.4 and the position of 2.20 Å obtained from the spin-polarized DFT. It is obvious that the changes in $g(r)$ due to the omission of the spin polarization are opposite to those observed in the experiments. We conclude from these results that the spin polarization has significant effects on the atomic structure of fluid Se at low densities $\leqslant$1.0 g cm^{-3} as well as on the electronic structure.

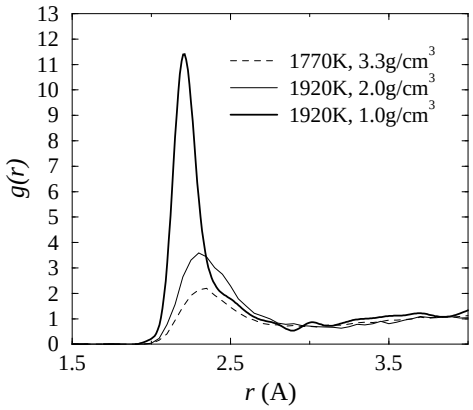

Figure 6. The pair distribution functions $g(r)$ of fluid Se. The dashed, thin solid and bold solid lines show the calculated results for (temperature (K), density (g cm^{-3})) = (1770, 3.33), (1920, 2.0) and (1920, 1.0), respectively.

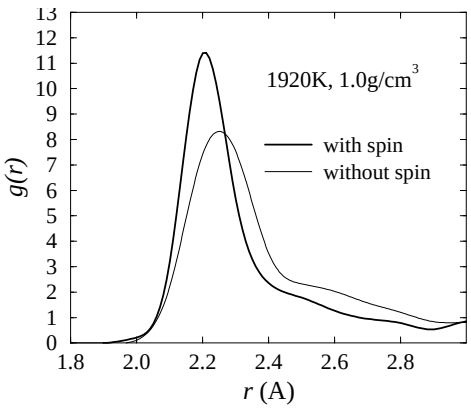

Figure 7. The pair distribution functions $g(r)$ of fluid Se for 1920 K and 1.0 g cm^{-3}. The bold and thin lines show $g(r)$ obtained from the spin-polarized and the spin-unpolarized DFTs, respectively.

To investigate the change of the chain structure in the supercritical region in detail, we obtain the Se–Se coordination number (n) distribution function $P(n)$, which is calculated simply by counting the number of Se atoms inside a sphere of radius R centred at each Se atom. Figure 8 displays the density dependence of $P(n)$. We use $R = 2.7$ Å. Although $P(n)$ depends somewhat on the value of R, the qualitative features of $P(n)$ never change. At all densities, the value of $P(3)$ is very small, which shows that fluid Se preserves the chain structure. With decreasing density, $P(2)$ decreases, while $P(1)$ increases. This indicates the shortening of Se chains. At the density of 1.0 g cm^{-3}, $P(2)$ is almost half of $P(1)$; this results from the presence of a large number of Se_2 dimers.

To see the chain-length distribution related to the density, we decompose the system into an assembly of twofold-coordinated chains. If the distance between the two Se atoms is smaller than R, we suppose that they share a bond and belong to the same chain. Figure 9 shows the chain-length distribution function $L(N)$, with N being the number of atoms per chain. In the semiconducting phase (3.75 g cm^{-3}), $L(N)$ is distributed over a large number of atoms $N > 20$. In the metallic phase (3.33 g cm^{-3}), $L(N)$ is distributed mainly over up to $N = 10$ atoms and, in the supercritical phases, the distribution of $L(N)$ is restricted to smaller N. At the density of 1.0 g cm^{-3}, $L(N)$ has finite values only up to $N = 6$, and more than half of the Se atoms form Se_2 dimers.

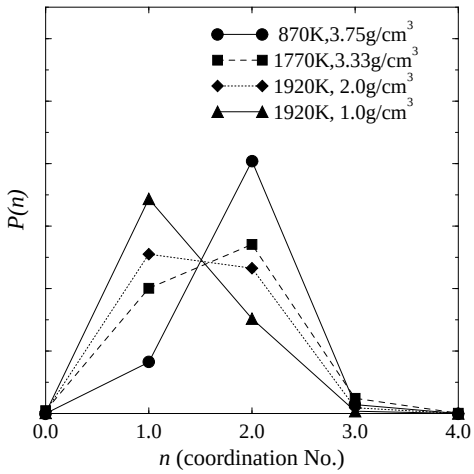

Figure 8. The Se–Se coordination number (n) distribution function $P(n)$ of fluid Se. The circles, squares, diamonds and triangles show the calculated results for (temperature (K), density (g cm^{-3})) = (870, 3.75), (1770, 3.33), (1920, 2.0) and (1920, 1.0), respectively.

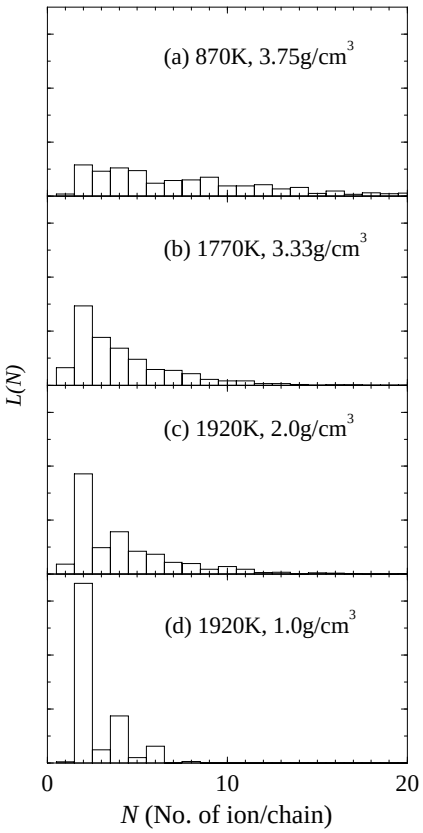

Figure 9. The chain-length distribution function $L(N)$, with N being the number of atoms per chain, of fluid Se for (temperature (K), density (g cm^{-3})) = (a) (870, 3.75), (b) (1770, 3.33), (c) (1920, 2.0) and (d) (1920, 1.0).

3.4. Spatial distribution of the spin density

As described in the preceding sections, the spin polarization plays an extremely important role in determining the electronic and atomic structures of supercritical fluid Se. In this section, we investigate the distribution of the spin density $\sigma(\boldsymbol{r})$ in the chain structure. The spatial

distributions of $\sigma(\boldsymbol{r})$ as well as the atomic configurations in the MD cell for two densities, 2.0 and 1.0 g cm^{-3}, are displayed in figures 10(a) and 10(b), respectively. The frame in each figure shows the supercell, and the size of the frame is proportional to that of the supercell. Two Se atoms, whose distance apart is smaller than 2.7 Å, are connected by the bond.

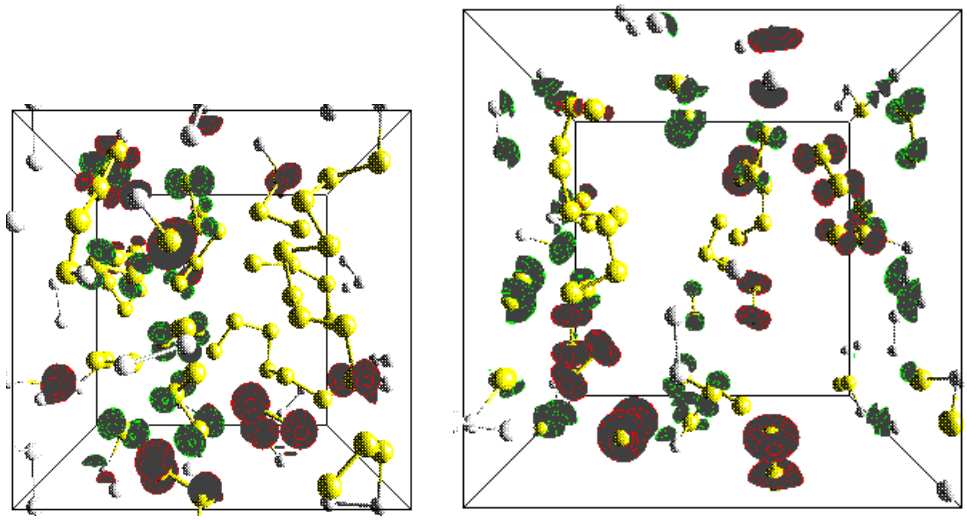

Figure 10. The atomic configuration and spatial distribution of the spin density $\sigma(\boldsymbol{r})$ of fluid Se for two densities: (a) 2.0 and (b) 1.0 g cm^{-3}. The frame shows the supercell, and the size of the frame is proportional to that of the supercell. Two Se atoms, whose distance apart is smaller than 2.7 Å, are connected by the bond. The contour surfaces are drawn for the spin density of 0.01 au.

It is seen from figure 10(a) that, at the density of 2.0 g cm^{-3}, the Se atoms have a chain structure, and that $\sigma(\boldsymbol{r})$ distributes mainly around the end of the Se chains. From figure 10(b), we can see that, at the density of 1.0 g cm^{-3}, almost half of the Se atoms form dimers and the rest are present in short chains. The distributions of the $\sigma(\boldsymbol{r})$ around the dimers have dumb-bell-shaped distributions similar to that around an isolated dimer. In both states, there is a strong correlation between the chain structure and the amount of spin polarization around each Se atom; two Se atoms from the ends of each Se chain, including dimers, have large spin polarization, while other Se atoms, i.e. those in the middle of the Se chains, have small or almost zero spin polarization.

4. Summary

In this paper, we have investigated the effects of spin polarization on the atomic and electronic structures of supercritical fluid Se by means of *ab initio* molecular-dynamics simulations using the fully spin-polarized and generalized-gradient-corrected density functional theory. Two simulations have been carried out at different densities $d = 2.0$ and 1.0 g cm^{-3} (cf. the critical density $d_c = 1.85$ g cm^{-3}) in the supercritical region, thus supplementing the previous simulations for the semiconducting and metallic phases. By investigating the density dependence of the electronic density of states and the pair distribution functions, it is shown that the spin polarization plays an extremely important role in determining the electronic and

atomic structures of supercritical fluid Se with low densities $d < d_c$. If the spin polarization is taken into account in the theory, the metal–insulator transition in supercritical fluid Se is successfully reproduced, and the structural changes are consistent with the experimental observations. From the spatial distribution of the spin density, it is confirmed that there is a strong correlation between the chain structure and the amount of spin polarization around each Se atom.

Acknowledgments

We are grateful to Professor K Tamura and Professor M Inui for useful discussions. This work was supported by a Grant-in-Aid for Scientific Research on Priority Areas (No 07236102) from the Ministry of Education, Science, Sports and Culture, Japan. The authors thank the Supercomputer Centre, Institute for Solid State Physics, University of Tokyo, for the use of the FACOM VPP500.

References

[1] Gerlach E and Grosse P (ed) 1979 *Proc. Int. Conf. on the Physics of Selenium and Tellurium (Königstein, Germany, 1979)* (Berlin: Springer)
[2] Perron J C, Rabit J and Rialland J F 1982 *Phil. Mag.* B **46** 321
[3] Freyland W and Cutler M 1980 *J. Chem. Soc. Faraday Trans.* **76** 756
[4] Hoshino H, Schmutzler R W and Hensel F 1976 *Ber. Bunsenges. Phys. Chem.* **80** 27
[5] Hoshino H, Schmutzler R W, Warren W W Jr and Hensel F 1976 *Phil. Mag.* B **33** 255
[6] Hosokawa S and Tamura K 1990 *J. Non-Cryst. Solids* **117+118** 52
[7] Warren W W Jr and Dupree R 1980 *Phys. Rev.* B **22** 2257
[8] Tamura K 1996 *J. Non-Cryst. Solids* **205–207** 239
[9] Inui M, Noda T and Tamura K 1996 *J. Non-Cryst. Solids* **205–207** 261
[10] Shimojo F, Hoshino K, Watabe M and Zempo Y 1998 *J. Phys.: Condens. Matter* **10** 1199
[11] Inui M, Tamura K, Hazemann J L, Raoux D, Soldo Y and Argoud R 1999 *J. Non-Cryst. Solids* at press
[12] Tamura K and Inui M 1999 *MRS Bull.* **24** 26
[13] Hohl D and Jones R O 1991 *Phys. Rev.* B **43** 3856
[14] Kirchhoff F, Kresse G and Gillan M J 1998 *Phys. Rev.* B **57** 10 482
[15] Kresse G, Kirchhoff F and Gillan M J 1999 *Phys. Rev.* B **59** 3501
[16] Perdew J P 1991 *Electronic Structure of Solids '91* ed P Ziesche and H Eschrig (Berlin: Akademie)
Perdew J P, Chevary J A, Vosko S H, Jackson K A, Pederson M R, Singh D J and Fiolhais C 1992 *Phys. Rev.* B **46** 6671
[17] Shimojo F, Zempo Y, Hoshino K and Watabe M 1995 *Phys. Rev.* B **52** 9320
[18] Arias T A, Payne M C and Joannopoulos J D 1992 *Phys. Rev.* B **45** 1538
[19] Kresse G and Hafner J 1994 *Phys. Rev.* B **49** 14 251
[20] Vanderbilt D 1990 *Phys. Rev.* B **41** 7892
[21] Kresse G and Hafner J 1994 *J. Phys.: Condens. Matter* **6** 8245
[22] Nosé S 1984 *Mol. Phys.* **52** 255
[23] Hoover W G 1985 *Phys. Rev.* A **31** 1695
[24] Cherin P and Unger P 1967 *Inorg. Chem.* **6** 1589
[25] Katayama Y, Yao M, Ajiro Y, Inui M and Endo H 1989 *J. Phys. Soc. Japan* **58** 1811
[26] Shimojo F, Hoshino K and Zempo Y 1998 *J. Phys.: Condens. Matter* **10** L177
[27] Ohtani H, Yamaguchi T and Yonezawa F 1998 *J. Phys. Soc. Japan* **67** 2807